

RESEARCH LETTER

10.1002/2016GL067987

Key Points:

- We identify a large increase in U.S. methane emissions over the past decade
- Increase occurred during a time when emission inventories indicate no change in U.S. emissions
- The U.S. could account for 30–60% of the global increase in atmospheric methane over the past decade

Supporting Information:

- Supporting Information S1

Correspondence to:

D. J. Jacob,
djjacob@fas.harvard.edu

Citation:

Turner, A. J., D. J. Jacob, J. Benmergui, S. C. Wofsy, J. D. Maasakkers, A. Butz, O. Hasekamp, and S. C. Biraud (2016), A large increase in U.S. methane emissions over the past decade inferred from satellite data and surface observations, *Geophys. Res. Lett.*, 43, 2218–2224, doi:10.1002/2016GL067987.

Received 26 JAN 2016

Accepted 2 FEB 2016

Accepted article online 6 FEB 2016

Published online 2 MAR 2016

Corrected 2 MAR 2016

This article was corrected on 2 MAR 2016. See the end of the full text for details.

©2016. The Authors.

This is an open access article under the terms of the Creative Commons Attribution-NonCommercial-NoDerivs License, which permits use and distribution in any medium, provided the original work is properly cited, the use is non-commercial and no modifications or adaptations are made.

A large increase in U.S. methane emissions over the past decade inferred from satellite data and surface observations

A. J. Turner¹, D. J. Jacob^{1,2}, J. Benmergui¹, S. C. Wofsy^{1,2}, J. D. Maasakkers¹, A. Butz³, O. Hasekamp⁴, and S. C. Biraud⁵
¹School of Engineering and Applied Sciences, Harvard University, Cambridge, Massachusetts, USA, ²Department of Earth and Planetary Sciences, Harvard University, Cambridge, Massachusetts, USA, ³IMK-ASF, Karlsruhe Institute of Technology, Karlsruhe, Germany, ⁴Netherlands Institute for Space Research, Utrecht, Netherlands, ⁵Earth Sciences Division, Lawrence Berkeley National Laboratory, Berkeley, California, USA

Abstract The global burden of atmospheric methane has been increasing over the past decade, but the causes are not well understood. National inventory estimates from the U.S. Environmental Protection Agency indicate no significant trend in U.S. anthropogenic methane emissions from 2002 to present. Here we use satellite retrievals and surface observations of atmospheric methane to suggest that U.S. methane emissions have increased by more than 30% over the 2002–2014 period. The trend is largest in the central part of the country, but we cannot readily attribute it to any specific source type. This large increase in U.S. methane emissions could account for 30–60% of the global growth of atmospheric methane seen in the past decade.

1. Introduction

Methane is the second most important anthropogenic greenhouse gas, with a radiative forcing of 0.97 W m^{-2} since preindustrial times on an emission basis, as compared to 1.68 W m^{-2} for CO_2 [Intergovernmental Panel on Climate Change (IPCC), 2013]. The global burden of atmospheric methane rose by $1\text{--}2\% \text{ a}^{-1}$ in the 1970s and 1980s, stabilized in the 1990s [Dlugokencky, 2003], and has been rising again since the mid-2000s [Rigby et al., 2008; Dlugokencky et al., 2009]. There has been much speculation as to the cause for the recent trends with explanations including oil and gas production [Wang et al., 2004; Aydin et al., 2011; Simpson et al., 2012; Bruhwiler et al., 2014; Franco et al., 2015], microbial sources [Kai et al., 2011; Levin et al., 2012], wetlands [Dlugokencky et al., 2009; Bousquet et al., 2011; Pison et al., 2013; Bergamaschi et al., 2013], and changes in the OH sink [Fiore et al., 2006; Rigby et al., 2008]. Here we show evidence from atmospheric observations to suggest that U.S. methane emissions have increased by more than 30% over the past decade, which would represent a major contribution to the global increase of methane concentrations.

Major anthropogenic sources of atmospheric methane include oil and gas systems, livestock (enteric fermentation and manure management), coal mining, and waste (landfills and wastewater). Wetlands are the dominant natural source. Oxidation by the hydroxyl radical is the main sink of methane, imposing an atmospheric lifetime of about 10 years [IPCC, 2013; Kirschke et al., 2013]. The current global source of methane is constrained to $550 \pm 60 \text{ Tg a}^{-1}$ from knowledge of the global sink [Prather et al., 2012]. However, estimating the contributions from different source types and regions is difficult due to spatial overlap in the sources and because sources mostly involve biological processes and fossil fuel losses that are hard to quantify [Dlugokencky et al., 2011].

Methane emissions can be estimated using “bottom-up” methods that compute emissions as the product of activity rates (e.g., number of gas wells drilled) and emission factors per unit of activity (e.g., methane emission per well drilled), thus relating emissions to the underlying physical processes. Emission factors often have large uncertainties. Bottom-up estimates can be tested by “top-down” methods that use atmospheric observations of methane to constrain emissions on the basis of a chemical transport model relating emissions to concentrations. Inverse studies optimize emission estimates by combining bottom-up and top-down constraints, often using Bayesian inference.

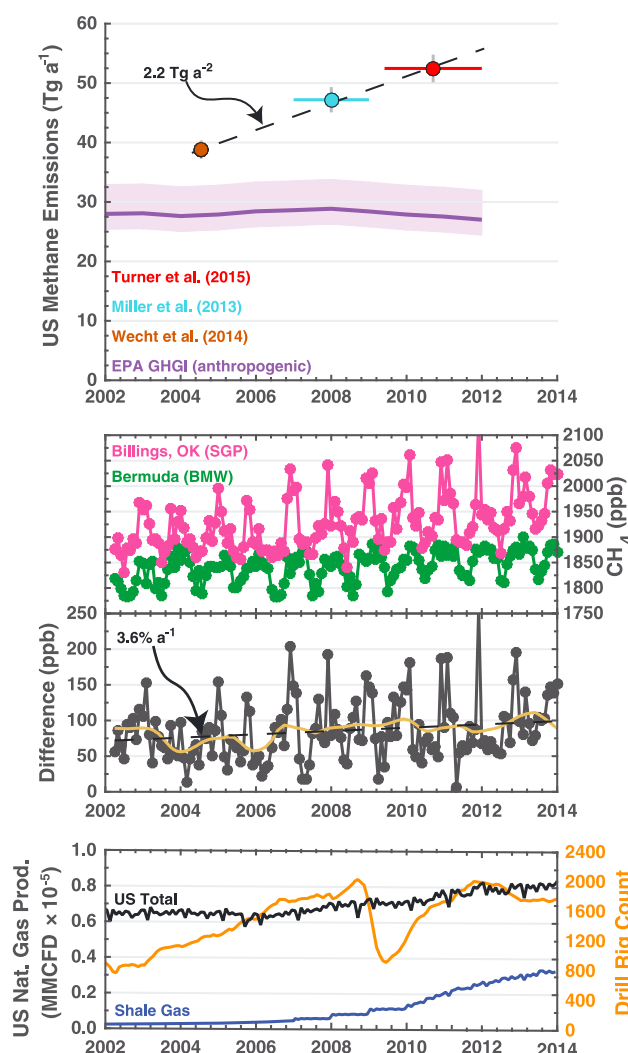


Figure 1. The 2002–2014 trends in U.S. methane emissions, atmospheric mixing ratios, and gas production rates. (top) The total contiguous U.S. (CONUS) methane emissions from three recent inverse studies [Miller et al., 2013; Wecht et al., 2014; Turner et al., 2015] with horizontal bars indicating the temporal averaging periods and vertical bars indicating reported uncertainties. U.S. EPA anthropogenic emission estimates from the Greenhouse Gas Inventory for 2002–2012 are also shown, with shading indicating reported uncertainties [US EPA, 2014]. (middle) The monthly atmospheric methane mixing ratios measured in surface air by the U.S. DOE at the Southern Great Plains site [SGP; Biraud et al., 2013] near Billings, Oklahoma (36.62°N , 97.48°W) and the NOAA/ESRL site (BMW) [NOAA ESRL, 2015] at Bermuda (32.27°N , 64.87°W), along with the corresponding SGP-BMW difference (black), a deseasonalized difference (gold line), and the ordinary least squares trend expressed as the percent change from 2004 (dashed black line). (bottom) The trend in CONUS oil and gas production and drilling activity as measured by active rig counts [US EIA, 2015] (number of active rigs at a given time). Oil and gas production data are from the U.S. Energy Information Administration.

2. U.S. Methane Emissions

The Greenhouse Gas Inventory of the U.S. Environmental Protection Agency [US EPA, 2014] provides the most detailed bottom-up estimate of U.S. anthropogenic methane emissions, following IPCC guidelines for reporting [Eggleston et al., 2006]. Figure 1 shows yearly emissions from 2002 to 2012. Values vary between 27.0 and 28.9 Tg a^{-1} over the period with no significant trend. Over 98% of emissions are in the contiguous U.S. (CONUS), excluding Alaska, Hawaii, and Puerto Rico [Maasakkers et al., 2015]. The EDGAR v4.2FT2010 global inventory [European Commission, 2013] also shows no significant trend in U.S. emissions from 2002 to 2010 (see Figure S10 in the supporting information). Major contributions in the U.S. EPA inventory and their interannual ranges are 30–32% from oil and gas, 31–34% from livestock, 21–22% from waste, and 10–13% from coal. Natural wetland emissions in CONUS are estimated to be $8.5 \pm 5 \text{ Tg a}^{-1}$ for 1993–2004 based on

the Wetland CH₄ Inter-comparison of Models Project ensemble of bottom-up models [Melton *et al.*, 2013; Wania *et al.*, 2013].

Recent work by Wecht *et al.* [2014], Miller *et al.* [2013], and Turner *et al.* [2015] used inverse methods to derive CONUS methane emissions of 38.8 ± 1.3 , 47.2 ± 1.9 , and 52.5 ± 2.1 Tg a⁻¹, respectively. Wecht *et al.* [2014] used Scanning Imaging Absorption Spectrometer for Atmospheric Chartography (SCIAMACHY) satellite data for July–August 2004. Miller *et al.* [2013] used NOAA Global Greenhouse Gas Reference Network in situ observations for 2007–2008 from ground stations and aircraft. Turner *et al.* [2015] used Greenhouse Gases Observing Satellite (GOSAT) data for June 2009 to December 2011. Wecht *et al.* [2014] found the total CONUS anthropogenic emissions to be consistent with the U.S. EPA bottom-up estimates, while Miller *et al.* [2013] and Turner *et al.* [2015] found much higher values. All three found maximum emissions in the South Central U.S., a region with large sources from livestock and oil and gas production. The reported uncertainties in these studies are likely too low because they do not properly account for systematic errors [Peylin, 2002; Heald *et al.*, 2004; Ganesan *et al.*, 2014]. The U.S. EPA inventory gives only national totals, so pinpointing specific regions of discrepancy is difficult, and the spatial overlap between livestock and oil and gas sources makes it difficult to attribute the high South Central U.S. emissions to a specific source type [Turner *et al.*, 2015]. A spatially resolved version of the U.S. EPA inventory is currently under development [Maasakkers *et al.*, 2015].

A possible factor contributing to the difference in CONUS emissions between the three inverse modeling studies is the time period investigated, as shown in Figure 1. Treating the results of the inverse studies as a time series and applying a least squares regression implies an increasing trend of 2.2 Tg a⁻² in U.S. methane emissions. This corresponds to a 38% increase from 2004 to 2011 or a 5.4% a⁻¹. Natural gas production and drilling activity increased greatly during that period [US EIA, 2015] (Figure 1, bottom) though the U.S. EPA inventory indicates a 3% decrease in national oil and gas emissions over the period due to lower emission factors (better control of leaks).

3. Trends in U.S. Surface Observations

Long-term measurements of methane dry-air molar mixing ratios from the DOE/Atmospheric Radiation Measurement (ARM) Southern Great Plains (SGP) [Biraud *et al.*, 2013] site in central Oklahoma offer independent evidence of a CONUS emission trend. There are other surface sites in the CONUS (Figure S6), but SGP has one of the longest continuous records and is most centrally located. Figure 1 (middle) shows the 2002–2014 trend in the deseasonalized difference between methane measured at SGP and at the Tudor Hill Atmospheric Observatory in Bermuda (BMW) [NOAA ESRL, 2015], taken as a Northern Hemispheric background. The SGP-BMW difference shows a trend of 2.3 ppb a⁻¹ ($p < 0.01$) from 2002 to 2014 and 3.9 ppb a⁻¹ for the 2004–2011 period. This 2004–2011 period is relevant here because it is the time period covered by the inversion studies [Miller *et al.*, 2013; Wecht *et al.*, 2014; Turner *et al.*, 2015]. A similar trend is found when using the NOAA Mauna Loa Observatory site in Hawaii (MLO) [NOAA ESRL, 2015] as reference background (see Figure S7). We may expect the difference with SGP to reflect the footprint of U.S. emissions affecting SGP, which implies a relative increase in these emissions of 3.6% a⁻¹ for 2002–2014 and 6.0% a⁻¹ for the 2004–2011 time period covered by the inversion studies [Miller *et al.*, 2013; Wecht *et al.*, 2014; Turner *et al.*, 2015]. The 2004–2011 trend is larger because of the 2004 minimum apparent in Figure 1 and is consistent with the 5.4% a⁻¹ CONUS trend for 2004–2011 implied by the inverse studies, as might be expected since SGP is in the South Central U.S. where inverse studies point to large underestimates in emissions. Scaling the SGP-BMW difference correspondingly would suggest a CONUS trend in methane emissions of 3.2% a⁻¹ or 1.3 Tg a⁻² for 2002–2014.

Bruhwyler *et al.* [2014] previously used a global inversion of NOAA/ESRL surface data to derive 2000–2010 emission trends for large continental regions. They found a 4 Tg a⁻¹ increase in fossil fuel emissions from temperate North America (as defined by The Atmospheric Tracer Transport Model Intercomparison Project regions, which is larger than the CONUS) over that period (0.4 Tg a⁻²). This is a factor of 3–4 lower than what we derive. Their results showed an increasing residual difference in the simulation of SGP concentrations over the 2000–2010 period, suggesting a larger trend in CONUS emissions than derived in their inversion. Schneising *et al.* [2014] found from SCIAMACHY satellite data that methane emissions grew by 1.5 Tg a⁻¹ in the Bakken (North Dakota) and Eagle ford (Texas) oil and gas basins during 2006–2011, which alone would drive an increase of 5% a⁻¹ in CONUS methane emissions. Franco *et al.* [2015] reported a $4.90 \pm 0.91\%$ a⁻¹ rise of ethane concentrations over 2009–2014 at the Jungfraujoch

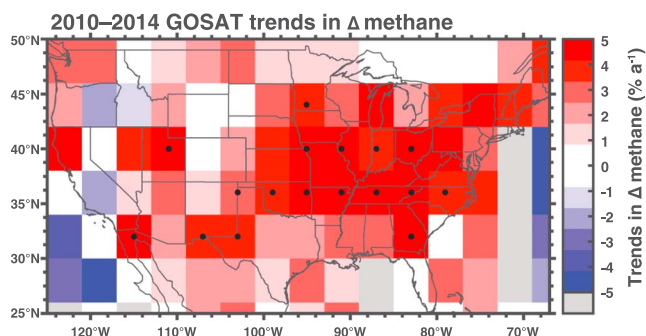


Figure 2. The 2010–2014 trend in U.S. methane enhancements as seen from GOSAT. The methane enhancement (Δ methane) is defined as the difference in the tropospheric column mixing ratio relative to the oceanic background measured in the glint mode over the North Pacific (176–128°W, 25–43°N) and normalized with the 2010 Δ methane. Trends are computed on a $4^\circ \times 4^\circ$ grid. Statistically significant trends ($p < 0.01$) are indicated by a dot.

sampling locations separated by 90–280 km along the orbit tracks. GOSAT has three observing modes: high gain (nominal setting over land), medium gain (setting over highly reflective surfaces), and ocean glint (setting over the ocean). We use RemoTeC v2.3.6 proxy methane retrievals [Butz *et al.*, 2011; Schepers *et al.*, 2012] (data available at <http://www.temis.nl/climate/methane.html>) in the high-gain nadir and ocean glint modes that pass all quality flags. The proxy methane retrieval method [Frankenberg *et al.*, 2006] assumes knowledge of the CO_2 concentration, and RemoTeC uses CO_2 concentrations from CarbonTracker including long-term trends [Peters *et al.*, 2007]. Validation with data from the Total Carbon Column Observing Network [Wunch *et al.*, 2011] shows that the RemoTeC retrieval has a single-scene precision of 14 ppb and a differential accuracy of 3 ppb [Buchwitz *et al.*, 2015].

GOSAT observations are spatially sparse, but they are temporally dense because the satellite always revisits the same ground pixels, every 3 days [Kuze *et al.*, 2009]. They are therefore well suited for temporal trend analyses. For example, the $4^\circ \times 4^\circ$ pixel encompassing SGP has 1937 data points from January 2010 to January 2014 (see Figure S15). We examined the spatial distribution of GOSAT CONUS trends from January 2010 to January 2014, using ocean glint retrievals over the North Pacific to subtract the background and correcting for spatial differences in tropospheric contributions to the total columns on the basis of local orography. We refer to the difference between CONUS methane and North Pacific background for the corresponding latitude as the enhancement (“ Δ methane”) due to U.S. emissions. Pacific air generally provides a good estimate of the U.S.

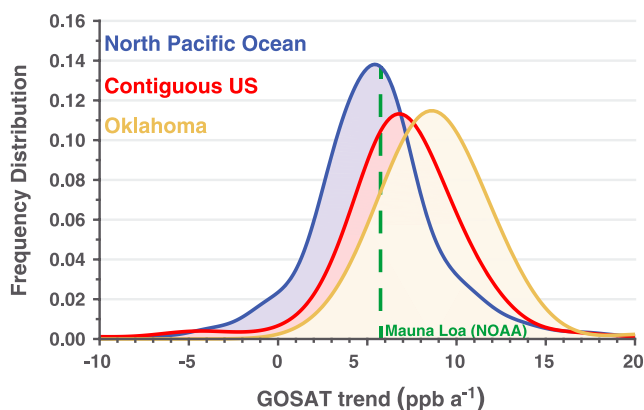


Figure 3. Spatial frequency distributions of 2010–2014 methane increases seen from GOSAT. Values are shown for the state of Oklahoma, the contiguous U.S. (CONUS), and the North Pacific (176–128°W, 25–43°N). The 2010–2014 trend at the NOAA Mauna Loa Observatory site (MLO) is also shown. GOSAT trends were computed on a $0.5^\circ \times 0.5^\circ$ grid, weighted by the square root of the number of retrievals, and distributions were computed with kernel density estimation.

European mountain site and pointed to the growth of North American shale gas exploitation as a possible explanation. Vinciguerra *et al.* [2015] found an increase of $\sim 6\% \text{ a}^{-1}$ in ethane concentrations in Maryland over 2010–2013 and attributed it to gas production in the Marcellus Shale upwind. They found no such increase in Atlanta, where there is no nearby oil and gas production.

4. Trends in GOSAT Satellite Data

The GOSAT satellite launched in Sun-synchronous low Earth orbit in January 2009 provides retrievals at

The GOSAT satellite launched in Sun-synchronous low Earth orbit in January 2009 provides retrievals at sampling locations separated by 90–280 km along the orbit tracks. GOSAT has three observing modes: high gain (nominal setting over land), medium gain (setting over highly reflective surfaces), and ocean glint (setting over the ocean). We use RemoTeC v2.3.6 proxy methane retrievals [Butz *et al.*, 2011; Schepers *et al.*, 2012] (data available at <http://www.temis.nl/climate/methane.html>) in the high-gain nadir and ocean glint modes that pass all quality flags. The proxy methane retrieval method [Frankenberg *et al.*, 2006] assumes knowledge of the CO_2 concentration, and RemoTeC uses CO_2 concentrations from CarbonTracker including long-term trends [Peters *et al.*, 2007]. Validation with data from the Total Carbon Column Observing Network [Wunch *et al.*, 2011] shows that the RemoTeC retrieval has a single-scene precision of 14 ppb and a differential accuracy of 3 ppb [Buchwitz *et al.*, 2015].

GOSAT observations are spatially sparse, but they are temporally dense because the satellite always revisits the same ground pixels, every 3 days [Kuze *et al.*, 2009]. They are therefore well suited for temporal trend analyses. For example, the $4^\circ \times 4^\circ$ pixel encompassing SGP has 1937 data points from January 2010 to January 2014 (see Figure S15). We examined the spatial distribution of GOSAT CONUS trends from January 2010 to January 2014, using ocean glint retrievals over the North Pacific to subtract the background and correcting for spatial differences in tropospheric contributions to the total columns on the basis of local orography. We refer to the difference between CONUS methane and North Pacific background for the corresponding latitude as the enhancement (“ Δ methane”) due to U.S. emissions. Pacific air generally provides a good estimate of the U.S. background at the corresponding latitude [Benmergui *et al.*, 2015]. To check the consistency in background trends between nadir and glint modes, we compared the two at southern mid-latitudes (using Patagonia for land) and found no significant differences (see Figure S5).

To obtain the orography-corrected Δ methane, we first normalize all the methane retrievals to account for variations in orography and tropopause height, similar to the approach of Kort *et al.* [2014]. The normalization is computed by determining the local (retrievals within a 300 km radial distance) relationship between column dry-air mole fraction (X_{CH_4}) in the GOSAT retrieval and the fraction of air

in the troposphere (F_{trop}), using all GOSAT retrievals within a 300 km radius. F_{trop} is computed from the tropopause pressure in the NCEP/NCAR reanalysis [Kalnay *et al.*, 1996] and the surface pressure used in the GOSAT retrieval.

In this manner we obtain the methane enhancement (Δ methane) over the CONUS relative to the North Pacific at the same latitude as a difference in tropospheric columns. We then computed a 2010–2014 ordinary least squares trend in Δ methane for each $4^\circ \times 4^\circ$ grid box. The horizontal resolution ($4^\circ \times 4^\circ$) was chosen to minimize the impact of smearing due to atmospheric transport (see supporting information).

Figure 2 shows the spatial distribution of trends in GOSAT methane enhancements over CONUS from 2010 to 2014. The trends are expressed as percentage changes relative to the mean 2010 Δ methane. Figure S14 shows the absolute trend in Δ methane. We find statistically significant ($p < 0.01$) increasing trends across the Midwest. Trends are weaker and/or insignificant in the West and over the eastern seaboard. Trends in Δ methane can be expected to be proportional to trends in CONUS emissions, and the corresponding emission trend averaged over the CONUS ($2.8 \pm 0.3\% \text{ a}^{-1}$) is comparable to those inferred in Figure 1 from the inverse studies and the surface sites.

Figure 3 shows the frequency distribution of GOSAT 2010–2014 trends for three selected regions: (1) the background North Pacific ($176^\circ\text{--}128^\circ\text{W}$, $25^\circ\text{--}43^\circ\text{N}$), (2) the CONUS, and (3) the state of Oklahoma (for relation to the SGP site). Also shown is the trend inferred from surface observations at the MLO site for 2010–2014. North Pacific GOSAT trends are consistent with MLO, providing a check on the background trend used in our analysis. Using a Metropolis-Hastings algorithm, we find that trends in the CONUS distribution are 1.7 ppb a^{-1} larger than the background, a significant difference ($p < 0.01$), corresponding to a relative increase in Δ methane of $2.5\% \text{ a}^{-1}$ over the 2010–2014 period. Trends in Oklahoma are 3.2 ppb a^{-1} larger than background, corresponding to a relative increase in Δ methane of $4.7\% \text{ a}^{-1}$.

5. Discussion

Long-term surface observations and satellite retrievals of atmospheric methane, interpreted directly and using inverse methods, point to an increase of more than 30% in U.S. methane emissions over the past decade. The increase is largest in the central part of the country. The U.S. has seen a 20% increase in oil and gas production [US EIA, 2015] and a ninefold increase in shale gas production from 2002 to 2014 (Figure 1, bottom), but the spatial pattern of the methane increase seen by GOSAT does not clearly point to these sources. More work is needed to attribute the observed increase to specific sources.

Kirschke *et al.* [2013] found that the renewed growth in atmospheric methane between 2005 and 2010 could be explained by a $17\text{--}22 \text{ Tg a}^{-1}$ increase in global methane emissions. Our results suggest that increasing U.S. anthropogenic methane emissions could account for up to 30–60% of this global increase. Other studies have pointed to tropical sources as a major driver for this increase [Bousquet *et al.*, 2011; Bergamaschi *et al.*, 2013]. Better understanding of U.S. anthropogenic methane emissions, particularly those from the livestock and oil and gas sectors, is obviously needed.

References

- Aydin, M., K. R. Verhulst, E. S. Saltzman, M. O. Battle, S. A. Montzka, D. R. Blake, Q. Tang, and M. J. Prather (2011), Recent decreases in fossil-fuel emissions of ethane and methane derived from firm air, *Nature*, *476*, 198–201, doi:10.1038/nature10352.
- Benmergui, J., et al. (2015), Integrating diverse observations of North American CH₄ into flux inversions in CarbonTrackerLagrange-CH₄, Abstract A33F-0245 presented at 2015 AGU Fall Meeting, AGU, San Francisco, Calif., 14–18 Dec.
- Bergamaschi, P., et al. (2013), Atmospheric CH₄ in the first decade of the 21st century: Inverse modeling analysis using sciamachy satellite retrievals and noaa surface measurements, *J. Geophys. Res. Atmos.*, *118*, 7350–7369, doi:10.1002/jgrd.50480.
- Biraud, S. C., M. S. Torn, J. R. Smith, C. Sweeney, W. J. Riley, and P. P. Tans (2013), A multi-year record of airborne CO₂ observations in the US Southern Great Plains, *Atmos. Meas. Tech.*, *6*(3), 751–763, doi:10.5194/amt-6-751-2013.
- Bousquet, P., et al. (2011), Source attribution of the changes in atmospheric methane for 2006–2008, *Atmos. Chem. Phys.*, *11*(8), 3689–3700, doi:10.5194/acp-11-3689-2011.
- Bruhwyler, L., E. Dlugokencky, K. Masarie, M. Ishizawa, A. Andrews, J. Miller, C. Sweeney, P. Tans, and D. Worthy (2014), Carbontracker-CH₄: An assimilation system for estimating emissions of atmospheric methane, *Atmos. Chem. Phys.*, *14*(16), 8269–8293, doi:10.5194/acp-14-8269-2014.
- Buchwitz, M., et al. (2015), The greenhouse gas climate change initiative (GHG-CCI): Comparison and quality assessment of near-surface-sensitive satellite-derived CO₂ and CH₄ global data sets, *Remote Sens. Environ.*, *162*, 344–362, doi:10.1016/j.rse.2013.04.024.
- Butz, A., et al. (2011), Toward accurate CO₂ and CH₄ observations from GOSAT, *Geophys. Res. Lett.*, *38*, L14812, doi:10.1029/2011GL047888.

Acknowledgments

This work was supported by the NASA Carbon Monitoring System and a Department of Energy (DOE) Computational Science Graduate Fellowship (CSGF) to A.J.T. Observations collected in the Southern Great Plains were supported by the Office of Biological and Environmental Research of the U.S. Department of Energy under contract DE-AC02-05CH11231 as part of the Atmospheric Radiation Measurement Program (ARM), ARM Aerial Facility, and Terrestrial Ecosystem Science Program. A.B. is supported by Deutsche Forschungsgemeinschaft through the Emmy-Noether programme, grant BU2599/1-1 (RemoTeC). GOSAT retrieval algorithm development and processing was partly funded by the ESA GHG-CCI project. We thank E. Dlugokencky for providing data from the MLO and BMW sites.

- Dlugokencky, E. J. (2003), Atmospheric methane levels off: Temporary pause or a new steady-state?, *Geophys. Res. Lett.*, *30*(19), 1992, doi:10.1029/2003GL018126.
- Dlugokencky, E. J., et al. (2009), Observational constraints on recent increases in the atmospheric CH₄ burden, *Geophys. Res. Lett.*, *36*, L18803, doi:10.1029/2009GL039780.
- Dlugokencky, E. J., E. G. Nisbet, R. Fisher, and D. Lowry (2011), Global atmospheric methane: Budget, changes and dangers, *Philos. Trans. R. Soc. A*, *369*(1943), 2058–2072, doi:10.1098/rsta.2010.0341.
- Eggleston, H., L. Buendia, K. Miwa, T. Ngara, and K. Tanabe (2006), 2006 IPCC guidelines for national greenhouse gas inventories, *Tech. Rep.*, The Natl. Greenhouse Gas Invent. Program., The Inter. Panel on Clim. Change, Hayama, Kanagawa, Japan.
- European Commission (2013), Global emissions EDGAR v4.2 ft2010 (October 2013). [Available at <http://edgar.jrc.ec.europa.eu/overview.php?v=42FT2010>.]
- Fiore, A. M., L. W. Horowitz, E. J. Dlugokencky, and J. J. West (2006), Impact of meteorology and emissions on methane trends, 1990–2004, *Geophys. Res. Lett.*, *33*, L12809, doi:10.1029/2006GL026199.
- Franco, B., et al. (2015), Retrieval of ethane from ground-based ftir solar spectra using improved spectroscopy: Recent burden increase above Jungfraujoch, *J. Quant. Spectrosc. Radiat. Transfer*, *160*, 36–49, doi:10.1016/j.jqsrt.2015.03.017.
- Frankenberg, C., J. F. Meirink, P. Bergamaschi, A. P. H. Goede, M. Heimann, S. Körner, U. Platt, M. van Weele, and T. Wagner (2006), Satellite cartography of atmospheric methane from SCIAMACHY on board Envisat: Analysis of the years 2003 and 2004, *J. Geophys. Res.*, *111*, D07303, doi:10.1029/2005JD006235.
- Ganesan, A. L., et al. (2014), Characterization of uncertainties in atmospheric trace gas inversions using hierarchical Bayesian methods, *Atmos. Chem. Phys.*, *14*(8), 3855–3864, doi:10.5194/acp-14-3855-2014.
- Heald, C. L., D. J. Jacob, D. B. A. Jones, P. I. Palmer, J. A. Logan, D. G. Streets, G. W. Sachse, J. C. Gille, R. N. Hoffman, and T. Nehrkorn (2004), Comparative inverse analysis of satellite (mopitt) and aircraft (trace-p) observations to estimate asian sources of carbon monoxide, *J. Geophys. Res.*, *109*, D23306, doi:10.1029/2004JD005185.
- Intergovernmental Panel on Climate Change (IPCC) (2013), *Climate Change 2013: The Physical Science Basis. Contribution of Working Group I to the Fifth Assessment Report of the Intergovernmental Panel on Climate Change*, edited by T. F. Stocker et al., 1535 pp., Cambridge Univ. Press, Cambridge, U. K., and New York, doi:10.1017/CBO9781107415324.
- Kai, F. M., S. C. Tyler, J. T. Randerson, and D. R. Blake (2011), Reduced methane growth rate explained by decreased Northern Hemisphere microbial sources, *Nature*, *476*(7359), 194–197, doi:10.1038/nature10259.
- Kalnay, E., et al. (1996), The NCEP/NCAR 40-year reanalysis project, *Bull. Am. Meteorol. Soc.*, *77*(3), 437–471, doi:10.1175/1520-0477(1996)077<0437:Tnyp>2.0.Co;2.
- Kirschke, S., et al. (2013), Three decades of global methane sources and sinks, *Nat. Geosci.*, *6*(10), 813–823, doi:10.1038/ngeo1955.
- Kort, E. A., C. Frankenberg, K. R. Costigan, R. Lindenmaier, M. K. Dubey, and D. Wunch (2014), Four corners: The largest US methane anomaly viewed from space, *Geophys. Res. Lett.*, *41*, 6898–6903, doi:10.1002/2014GL061503.
- Kuze, A., H. Suto, M. Nakajima, and T. Hamazaki (2009), Thermal and near infrared sensor for carbon observation Fourier-transform spectrometer on the greenhouse gases observing satellite for greenhouse gases monitoring, *Appl. Opt.*, *48*(35), 6716–33, doi:10.1364/AO.48.006716.
- Levin, I., C. Veidt, B. H. Vaughn, G. Brailsford, T. Bromley, R. Heinz, D. Lowe, J. B. Miller, C. Poß, and J. W. C. White (2012), No inter-hemispheric $\delta^{13}\text{C}_{\text{CH}_4}$ trend observed, *Nature*, *486*(7404), E3–E4, doi:10.1038/nature11175.
- Maasakkers, J. D., D. J. Jacob, M. P. Sulprizio, A. J. Turner, M. Weitz, T. Wirth, C. Hight, M. DeFigueiredo, and A. A. Bloom (2015), A gridded version of the epa national methane inventory, paper presented at 2015 International Emission Inventory Conference, San Diego, Calif., [Available at http://www.epa.gov/ttn/chief/conference/ei21/session4/maasakkers_pres.pdf.]
- Melton, J. R., et al. (2013), Present state of global wetland extent and wetland methane modelling: Conclusions from a model inter-comparison project (WETCHIMP), *Biogeosciences*, *10*(2), 753–788, doi:10.5194/bg-10-753-2013.
- Miller, S. M., et al. (2013), Anthropogenic emissions of methane in the United States, *Proc. Natl. Acad. Sci. U.S.A.*, *110*(50), 20,018–20,022, doi:10.1073/pnas.1314392110.
- NOAA ESRL (2015), *Carbon Cycle Greenhouse Gas Group*. [Available at <http://www.esrl.noaa.gov/gmd/dv/data/>.]
- Peters, W., et al. (2007), An atmospheric perspective on North American carbon dioxide exchange: Carbontracker, *Proc. Natl. Acad. Sci. U.S.A.*, *104*(48), 18,925–18,930, doi:10.1073/pnas.0708986104.
- Peylin, P. (2002), Influence of transport uncertainty on annual mean and seasonal inversions of atmospheric CO₂ data, *J. Geophys. Res.*, *107*(D19), 4385, doi:10.1029/2001JD000857.
- Pison, I., B. Ringeval, P. Bousquet, C. Prigent, and F. Papa (2013), Stable atmospheric methane in the 2000s: Key-role of emissions from natural wetlands, *Atmos. Chem. Phys.*, *13*(23), 11,609–11,623, doi:10.5194/acp-13-11609-2013.
- Prather, M. J., C. D. Holmes, and J. Hsu (2012), Reactive greenhouse gas scenarios: Systematic exploration of uncertainties and the role of atmospheric chemistry, *Geophys. Res. Lett.*, *39*, L09803, doi:10.1029/2012GL051440.
- Rigby, M., et al. (2008), Renewed growth of atmospheric methane, *Geophys. Res. Lett.*, *35*, L22805, doi:10.1029/2008GL036037.
- Schepers, D., et al. (2012), Methane retrievals from Greenhouse Gases Observing Satellite (GOSAT) shortwave infrared measurements: Performance comparison of proxy and physics retrieval algorithms, *J. Geophys. Res.*, *117*, D10307, doi:10.1029/2012JD017549.
- Schneising, O., J. P. Burrows, R. R. Dickerson, M. Buchwitz, M. Reuter, and H. Bovensmann (2014), Remote sensing of fugitive methane emissions from oil and gas production in North American tight geologic formations, *Earth's Future*, *2*, 548–558, doi:10.1002/2014EF000265.
- Simpson, I. J., M. P. Sulbaek Andersen, S. Meinardi, L. Bruhwiler, N. J. Blake, D. Helmig, F. S. Rowland, and D. R. Blake (2012), Long-term decline of global atmospheric ethane concentrations and implications for methane, *Nature*, *488*(7412), 490–494, doi:10.1038/nature11342.
- Turner, A. J., et al. (2015), Estimating global and North American methane emissions with high spatial resolution using GOSAT satellite data, *Atmos. Chem. Phys.*, *15*, 7049–7069, doi:10.5194/acp-15-7049-2015.
- US EIA (2015), Emissions of greenhouse gases in the U.S., Tech. Rep., U.S. Energy Inf. Admin, Washington, D. C.
- US EPA (2014), Inventory of U.S. greenhouse gas emissions and sinks: 1990–2012, Tech. Rep., U.S. Environ. Prot. Agency, Washington, D. C.
- Vinciguerra, T., S. Yao, J. Dadzie, A. Chittams, T. Deskins, S. Ehrman, and R. R. Dickerson (2015), Regional air quality impacts of hydraulic fracturing and shale natural gas activity: Evidence from ambient VOC observations, *Atmos. Environ.*, *110*, 144–150, doi:10.1016/j.atmosenv.2015.03.056.

- Wang, J. S., J. A. Logan, M. B. McElroy, B. N. Duncan, I. A. Megretskaya, and R. M. Yantosca (2004), A 3-D model analysis of the slowdown and interannual variability in the methane growth rate from 1988 to 1997, *Global Biogeochem. Cycles*, *18*, GB3011, doi:10.1029/2003GB002180.
- Wania, R., et al. (2013), Present state of global wetland extent and wetland methane modelling: Methodology of a model inter-comparison project (WETCHIMP), *Geosci. Model Dev.*, *6*(3), 617–641, doi:10.5194/gmd-6-617-2013.
- Wecht, K. J., D. J. Jacob, C. Frankenberg, Z. Jiang, and D. R. Blake (2014), Mapping of North American methane emissions with high spatial resolution by inversion of SCIAMACHY satellite data, *J. Geophys. Res. Atmos.*, *119*, 7741–7756, doi:10.1002/2014JD021551.
- Wunch, D., G. C. Toon, J. F. Blavier, R. A. Washenfelder, J. Notholt, B. J. Connor, D. W. Griffith, V. Sherlock, and P. O. Wennberg (2011), The Total Carbon Column Observing Network, *Philos. Trans. R. Soc. A*, *369*(1943), 2087–112, doi:10.1098/rsta.2010.0240.

Erratum

Edward Dlugokencky had been listed as an author on the submitted manuscript but was removed from the final published version by mutual agreement. His contribution has been described in the Acknowledgment.